Functional and Immunofluorescence Evaluations of Vascular and Neural Integrities in Urinary Bladder of Streptozotocin-Induced Diabetic Mice

Mi-Hye Kwon*, Min-Ji Choi*, Fang-Yuan Liu, Fitri Rahma Fridayana, Lashkari Niloofar, Guo Nan Yin, Ji-Kan Ryu

Department of Urology, Inha University College of Medicine, National Research Center for Sexual Medicine, Incheon, Korea

Purpose: To assess functional and structural changes in vascular and neural structures associated with diabetic bladder dysfunction (DBD) in the bladders of streptozotocin (STZ)-induced diabetic mice.
Methods: Eight-week-old C57BL/6 mice were injected with STZ at 50 mg/kg daily for 5 consecutive days. Catheters were inserted 12 weeks later, and 5 days after catheter placement bladder functions were assessed by conscious cystometry. Neurovascular and extracellular matrix marker changes in harvested urinary bladders were investigated by immunofluorescent staining. Body weights and fasting and postprandial blood glucose levels were measured 12 weeks after STZ injection.
Results: STZ-induced diabetic mice had significantly lower body weights and significantly higher blood glucose levels. Assessment of bladder function in STZ-induced diabetic mice revealed a nearly 3-fold increase in bladder capacity and intercontractile interval compared to controls. However, basal pressure, maximal bladder pressure, and threshold pressure were not significantly different. Morphological and structural analysis showed that STZ-induced diabetic mice had significantly reduced microvascular density in lamina propria (33% of the nondiabetic control values), and severely decreased nerve contents in the detrusor region (42% of the nondiabetic control values).
Conclusions: STZ-induced diabetic mice exhibit functional and structural derangements in urinary bladder. The present study provides a foundation and describes a useful means of evaluating the efficacies of therapeutic targets and exploring the detailed mechanism of DBD.

Keywords: Urinary bladder; Blood vessel; Nerve; Diabetes mellitus; Mouse

- *HIGHLIGHTS*
  - Diabetic induction causes microvascular impairment, remodeling of the extracellular matrix, and disruption of neurogenic detrusor activity, which contributes to diabetic bladder dysfunction.

Corresponding author: Ji-KanRyu https://orcid.org/0000-0003-0025-6025
Department of Urology, Inha University School of Medicine, National Research Center for Sexual Medicine, 366 Seohae-daero, Jung-gu, Incheon 22332, Korea
Email: rjk0929@inha.ac.kr
Co-corresponding author: Guo Nan Yin https://orcid.org/0000-0002-2512-7337
Department of Urology, Inha University School of Medicine, National Research Center for Sexual Medicine, 366 Seohae-daero, Jung-gu, Incheon 22332, Korea
Email: jksuh@inha.ac.kr
*Mi-Hye Kwon and Min-Ji Choi contributed equally to this study as co-first authors.
Submitted: June 29, 2022 / Accepted after revision: August 29, 2022

INTRODUCTION

Diabetic bladder dysfunction (DBD), sexual dysfunction, and urinary tract infection are the most common urologic complications of diabetes and affect more than 50% of both type 1 and type 2 diabetes patients [1,2]. DBD is considered a group of progressive symptoms characterized early by increased frequency, urgency, and even urge incontinence [3,4], and chronic DBD is characterized by loss of sensation and decompensation of the bladder, resulting in overflow incontinence and high residual volumes after voiding [5]. Blood glucose control is the first step in the treatment of DBD, but because available treatments for DBD are limited and inadequate, the prevalence of DBD in patients on oral hypoglycemic therapy remains as high as 25% [6,7]. Therefore, further understanding of the pathophysiology and molecular mechanisms of DBD is required.

Bladder mucosa is composed of transitional epithelium (urothelium), basement membrane, and lamina propria (LP) [8]. Structural analysis has revealed that the LP contains a rich neurovascular network, elastic fibers, and smooth muscle bundles (muscularis mucosa) [8-10], and recent studies suggest that increased cellular degeneration and necrosis of bladder mucosal cells may underlie bladder microvascular and nerves damage in diabetes [11]. In addition, microvascular injury may impair bladder innervation, alter detrusor function, and lead to urothelial dysfunction [12]. However, little is known about whether pathological changes in bladder function are determined by changes in the neurovascular function of mucosa. The majority of animal studies on DBD have focused on bladder function in streptozotocin (STZ) induced diabetic rats and less on the pathophysiology of organic bladder damage [13,14]. Recently, a 3-dimensional reconstruction study of a complete mounted mouse bladder neurovascular network provided a useful tool for assessing pathological changes in mouse urinary bladder [10].

Consequently, the aim of the present study was to assess bladder function in an STZ-induced mouse model of diabetes by suprapubic bladder catheterization and conscious cystometry. In addition, we also assessed morphological and structural changes in bladder mucosa and detrusor regions caused by diabetes by immunofluorescence staining and examined microvascular and neural changes in LP and detrusor muscle. Unlike other previous studies [13,14], a key point of this study was the assessment of DBD by comparing angiogenesis and neuropathology in the bladders of control and STZ-induced mice. It is hoped that this study will provide a foundation for further detailed studies on the pathophysiology of bladder dysfunction in diabetes.

MATERIALS AND METHODS

Animals and Treatments

A total of 44 eight-week-old male C57BL/6 mice (weight, 20–25 g; Orient Bio, Inc., Seongnam, Korea) were used in this study. Animal experiments were performed after obtaining approval from the Institutional Animal Care and Use Subcommittee of our university (approval number: 190813-661). Animal were monitored daily for health and behavior, and animals were fed sterilized commercial standard laboratory food and water. Mice were maintained at room temperature (23°C±2°C), 40%–60% relative humidity, under a 12-hour light/dark cycle and specific pathogen-free conditions. Animals were euthanized by 100% CO_2 gas exchange in a closed container at a CO_2 exchange rate of 10%–30% of container volume/min. Cardiac and respiratory cessation were confirmed before harvesting tissues [15]. Diabetes was induced in 8-week-old C57BL/6J mice by injecting STZ intraperitoneally (i.p.) (STZ, 50 mg/kg, Sigma-Aldrich, St. Louis, MO, USA) in saline for 5 consecutive days. Compared with a single high-dose STZ (200 mg/kg) induction, this low-dose STZ-induced minimal toxicity and significantly reduced mortality in the induced diabetic mice (DM), as described previously [16,17]. Twelve weeks after completing STZ injections (after induction), mice with a tail vein blood glucose level > 300 mg/dL and exhibiting a significant body weight reduction were considered to have DM. Fasting and postprandial blood glucose levels were determined using an Accu-Check blood glucose meter (Roche Diagnostics, Mannheim, Germany) [18].

Suprapubic Bladder Catheter Implantation and Conscious Cystometry

Twelve weeks after induction, mice were anesthetized with ketamine (100 mg/kg, Yuhan Corp., Seoul, Korea) and xylazine (5 mg/kg, Bayer Korea, Seoul, Korea) i.p. and placed supine on a thermoregulated surgical table. Bladders were exposed by a lower abdominal midline incision, and then domes were punctured to insert a PolyE 120 Tubing, (ID 0.015 inches [0.38 mm], OD 0.042 inches [1.09 mm]; Smiths Medical International Ltd., Minneapolis, MN, USA). Catheters were secured with sutures, tunneled subcutaneously (to leave an exposed end through an incision in the back of the neck), and heat-sealed [19].

Conscious cystometry was performed in metabolic cages 5

days after catheter implantation [19]. The exposed end of the catheter was opened and connected to a pressure transducer (Biopac Systems, Goleta, CA, USA), and saline (154 mmol/L NaCl) was infused into the bladder using a pump 0.6 mL/hr for one hour [19]. Maximum pressure (highest pressure during voiding), threshold pressure (pressure before voiding contraction), basal pressure (lowest pressure between voids), voiding pressure (average calculated pressure between voids), and systolic interval (time between voids) were recorded.

Bladder Tissue Preparation
Whole urinary bladders were harvested from age-matched treatment-naïve mice 5 days after bladder function evaluation, as described previously [10]. Tissues were fixed in 4% paraformaldehyde in phosphate buffer saline (PBS) for 24 hours at 4°C. After washing 3 times with PBS, samples were embedded in optimal cutting temperature compound, placed in a cryostat at -20°C for 20 minutes, and thick sectioned (12 μm) for full-thickness bladder staining.

Histological Examination
After washing several times with PBS, samples were immersed in 3% bovine serum albumin for 1 hour at room temperature to minimize nonspecific antibody binding, and incubated with antibodies to PECAM-1 (an endothelial cell marker; Millipore, Temecula, CA, USA; 1:50; Cat# MAB1398Z), NG2 chondroitin sulfate proteoglycan (a pericyte marker; Millipore; 1:50; Cat# ab5320), collagen I (Abcam, Cambridge, UK; 1:50; Cat# ab34710), E-cadherin (Abcam; 1:50; Cat# ab11512), tyrosine hydroxylase (TH, Abcam; 1:50; Cat# ab112), choline acetyltransferase (ChAT, Abcam; 1:50; Cat# ab18736), calcitonin-gene related peptide (CGRP, Abcam; 1:50; Cat# ab36001), and βIII-tubulin (a neuronal marker; Abcam; 1:100; Cat# ab107216) for 48 hours at 4°C. After washing several times with PBS, the samples were incubated with Donkey anti-Rabbit IgG H&L (DyLight 550) (Abcam; 1:50; Cat# ab98489), FITC Affinipure goat anti-Armenian hamster IgG (H+L) (Jackson ImmunoResearch Laboratories, Inc.; 1:50; Cat# 127-095-160), goat anti-rabbit IgG H&L (Alexa Fluor 488) (Abcam; 1:50; Cat# ab150081), rhodamine (TRITC) AffiniPure donkey anti-rat IgG (H+L) (Jackson ImmunoResearch Laboratories, Inc.; 1:50; Cat# 712-025-150), donkey anti-Sheep IgG (H+L) FITC (Thermofisher; 1:50; Cat# A16042), rhodamine (TRITC) AffiniPure donkey anti-Goat IgG (H+L) (Jackson ImmunoResearch Laboratories, Inc.; 1:50; Cat# 705-025-147), and Alexa Fluor

488-donkey anti-chicken IgY (IgG) (H+L) (Jackson ImmunoResearch Laboratories, Inc.; 1:50; Cat# 703-545-155). After washing several times with 1×PBST, the samples were mounted in media containing 4,6-diamidino-2-phenylindole (DAPI) (Vector Laboratories, Inc.; Burlingame, California, US; Cat# H-1500) to stain nuclei. Sections were visualized, and images were obtained using a confocal microscope (K1-Fluo, Nanoscope Systems, Inc., Daejeon, Korea), and quantitative analysis was performed using an image analyzer system (Image J 1.34, National Institutes of Health, Bethesda, MD, USA; http://rsbweb.nih.gov/ij/).

Statistical Analysis
Results are expressed as the means ± standard error of the means of at least 4 independent experiments. The unpaired t-test was used to compare groups. The analysis was conducted using GraphPad Prism version 8 (Graph Pad Software, Inc., San Diego, CA, USA), and statistical significance was accepted for P-values < 0.05.

RESULTS

Metabolic Variables
Twelve weeks after completing STZ injections (after induction), fasting and postprandial blood glucose concentrations in mice were significantly higher in DM than in controls. In addition, mean body weight was significantly lower in DM (Table 1).

Bladder Function Evaluations in DM and Controls
Bladder function was assessed in age-matched controls and in DM 5 days after catheter implantation (performed 12 weeks after induction) by conscious cystometry to obtain urodynamic parameters, as previously described [19]. Bladder enlargement appeared to be part of DBD [20], however, the underlying

Table 1. Physiologic and metabolic parameters: 12 weeks after the final STZ injection

Variable	Control	STZ-induced DM
Body weight (g)	30.88 ± 0.26	24.2 ± 0.29*
Fasting glucose (mg/dL)	102.4 ± 1.43	543.8 ± 15.83*
Postprandial glucose (mg/dL)	178.8 ± 8.32	580.8 ± 16.07*

Values are the mean ± standard error of the mean for n = 5 animals per group.
STZ, streptozotocin; DM, diabetic mice.
*P < 0.01 vs. control group.

mechanism of diabetes-related bladder enlargement is largely unknown. In the present study we also demonstrated that compared with age-matched controls, the bladders of DM were significantly enlarged (Fig. 1A). The urination pattern of normal mice is regular and stable. However, urination frequency was significantly reduced in DM (Fig. 1B), and thus, the intercontractile interval (time between voids) was significantly greater in DM. On the other hand, basal pressure (lowest average pressure between voids), maximal bladder pressure (peak pressure during micturition), and threshold pressure (pressure immediately before micturition) were not significantly changed (Fig. 1C–F). These results confirmed that bladder dysfunction was significantly induced in DM.

Bladder Mucosa Microvascular Density Was Severely Decreased in DM

Bladder mucosa, especially the LP, possesses a rich vascular network, which plays a fundamental role in the exchange of molecules across the bladder wall [21]. Therefore, to determine whether the microvascular characteristics of the LP were altered in DM, we performed immunofluorescence staining for

PECAM-1 (an endothelial cell marker) and NG2 (a pericyte marker) in the bladders of DM and age-matched controls. We found that bladder LPs were rich in blood vessels, which concurs with previous studies [21]. In addition, endothelial cell and pericyte contents in the LPs of DM were significantly lower than in age-matched controls (Fig. 2). These results suggested that the effects of STZ on bladder microvasculature are similar to the deficits observed in diabetic retinopathy, nephropathy, and peripheral neuropathy.

Severe Thinning and Reduction of Extracellular Matrix in the Lamina Propria of DM

Urothelium rests upon LP, and extracellular matrix (ECM) provides nutritive and informative support for cells, and collagen is the main structural protein of bladder ECM [22,23]. Immunofluorescence staining for collagen I (suburothelial layer) and E-cadherin (a urothelial cell-adhesion marker) were performed in DM and control bladders to determine whether the urothelial layer in LP is altered under diabetic conditions. We found that collagen I expression was significantly diminished in the suburothelial layer of diabetic bladders (Fig. 3A, B). Although no
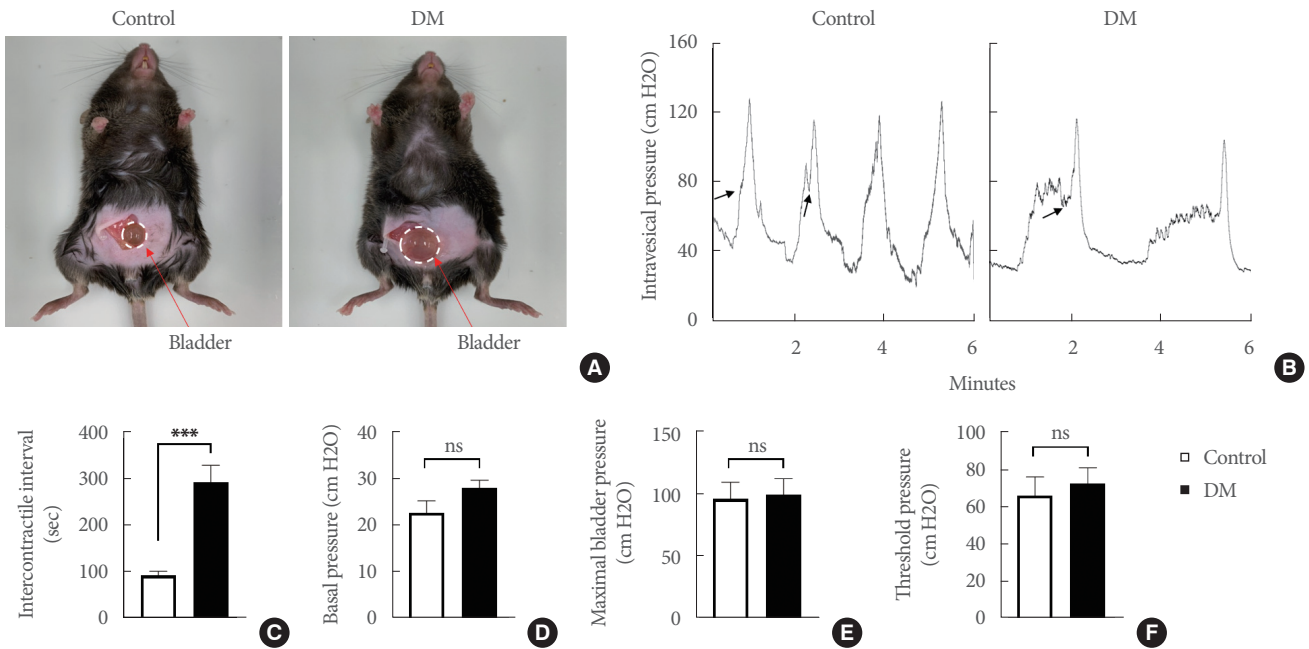
Fig. 1. Analysis of bladder function by conscious cystometry in streptozotocin (STZ)-induced diabetic mice (DM) and age-matched controls. (A) Representative bladder size as showed with white dotted circle in diabetic mice compared with age-matched control. (B) Representative traces of intravesical pressure in an awake, freely moving mouse 5 days after catheter implantation. Traces show 2–4 repeatable voiding cycles every 6 minutes. Comparison of cystometric parameters of intercontractile intervals (C), basal pressure (D), maximal bladder pressure (E), and threshold pressure (F, indicated by arrows). Results are presented as means ± standard error of the means (n = 6; ***P < 0.001, Student t-test). ns, not significant.

significant change in urothelial E-cadherin content was observed between normal and diabetic urinary bladder, we observed the area (as indicated by the arrow and elliptical yellow dotted line) of disrupted E-cadherin-positive urothelial linings in DM (Fig. 3A, C), which contributes to the decreased barrier function.
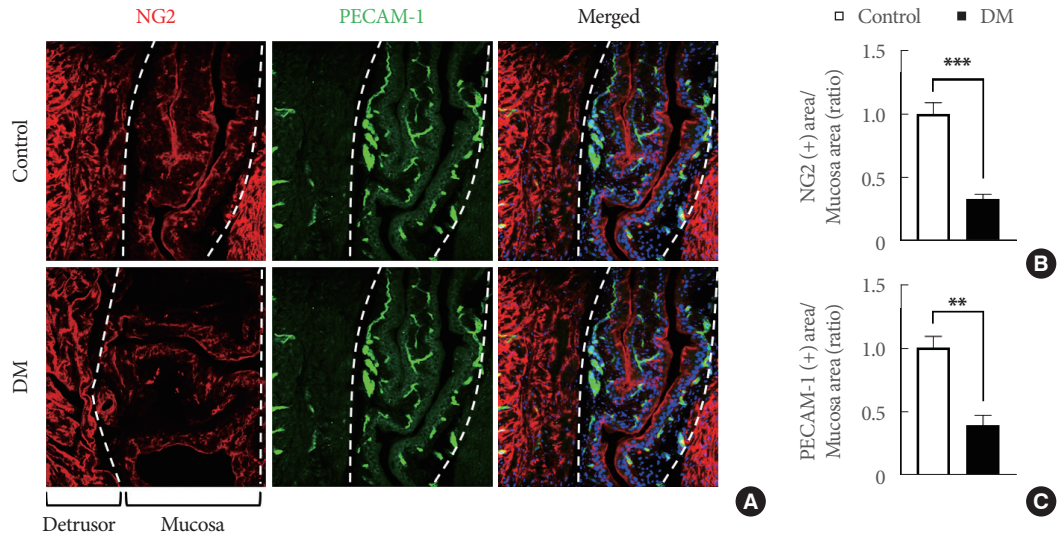

Fig. 2. Bladder mucosa microvascular structure was severely damaged in streptozotocin (STZ)-induced diabetic mice (DM). (A) NG2 (red) and PECAM-1 (green) immunostaining in bladder tissue mucosa from an STZ-induced diabetic mouse and an age-matched control. Nuclei were labeled with 4,6-diamidino-2-phenylindole (blue). Scale bars, 100 μm. Quantification of NG2 (B) and PECAM-1 (C) expressions in bladder mucosa (measured areas are indicated by dotted lines) using Image J (National Institutes of Health, Bethesda, MD, USA). Results are presented as means ± standard error of the means (n = 4; **P < 0.01, ***P < 0.001, Student t-test). Areas are presented as ratios versus controls.
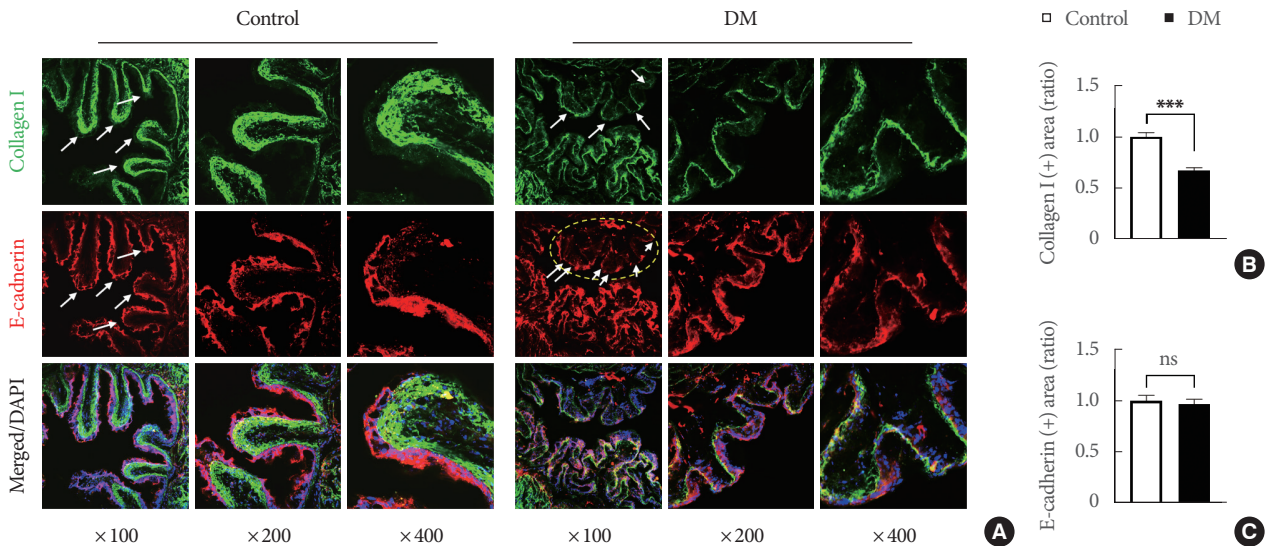

Fig. 3. Bladder lamina propria extracellular matrix was significantly thinner in streptozotocin (STZ)-induced diabetic mice (DM). (A) Collagen I (red) and E-cadherin (green) immunostaining in lamina propria (arrowed) and bladder tissues of an STZ-induced diabetic mice and an age-matched control. Nuclei were labeled with 4,6-diamidino-2-phenylindole (blue). Original magnification ×100 (left), ×200 (center), and ×400 (right). Quantifications of collagen I (B) and E-cadherin (C) expression in bladder lamina propria using Image J (National Institutes of Health, Bethesda, MD, USA). Results are presented as means ± standard error of the means (n = 4; ***P < 0.001, Student t-test). Areas are presented as ratios versus controls. ns, not significant.
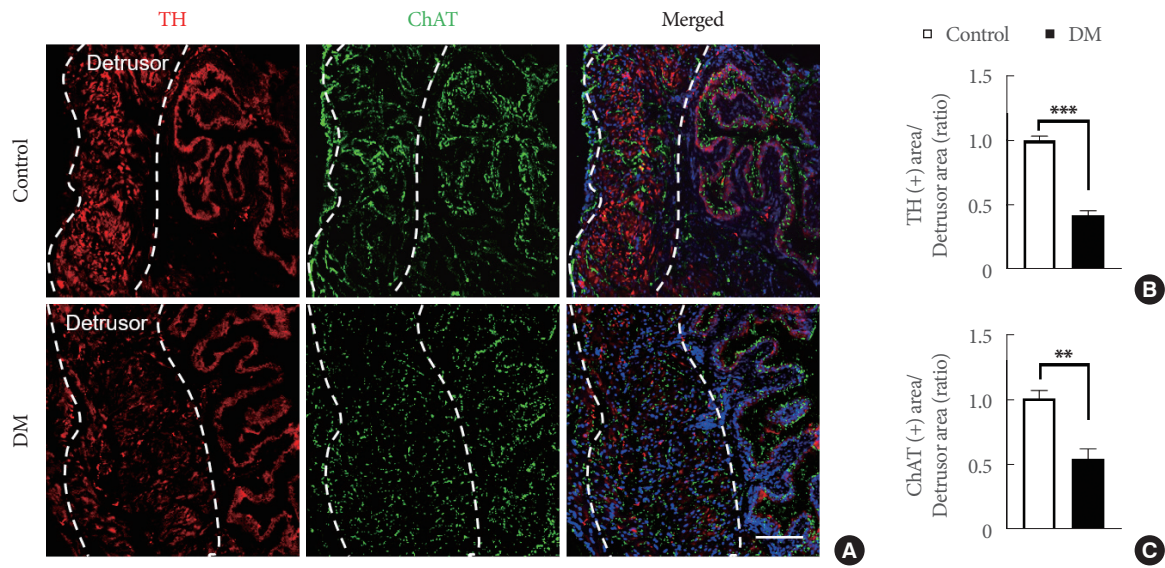
Fig. 4. Efferent nerve integrity was severely damaged in the bladder detrusor muscles of streptozotocin (STZ)-induced diabetic mice (DM). (A) Representative tyrosine hydroxylase (TH, red) and choline acetyltransferase (ChAT, green) immunostaining in bladder detrusor muscle of an STZ-induced diabetic mouse and an age-matched control (areas were measured inside the dotted lines). Nuclei were labeled with 4,6-diamidino-2-phenylindole (blue). Scale bars, 100 μm. Quantifications of TH (B) and ChAT (C) expressions in bladder detrusor muscle using Image J (National Institutes of Health, Bethesda, MD, USA). Results are presented as means ± standard error of the means (n = 4; **P < 0.01, ***P < 0.001, Student t-test). Results are presented as ratios versus controls.

Neurogenic Detrusor Action Was Severely Damaged in DM

Under normal conditions, the bladder stores and expels urine in a coordinated, controlled manner as regulated by the central and peripheral nervous systems [24]. Immunofluorescence staining for TH (a classical marker of presynaptic sympathetic innervation) and ChAT (a biochemical marker of cholinergic neurons) were used to evaluate whether efferent nerves (sympathetic and parasympathetic nerves) in the detrusor were altered under diabetic conditions. TH and ChAT expressions were significantly lower in diabetic bladder detrusor muscles (Fig. 4). In addition, immunofluorescence staining for CGRP (sensory afferent nerve) and βIII-tubulin were performed to investigate the effect of STZ-induced diabetes on afferent nerves. We found that CGRP and βIII-tubulin expressions were significantly reduced in the detrusor muscles of diabetic mouse bladders as compared with age-matched controls (Fig. 5).

DISCUSSION

The typical symptoms of DBD are dysesthesia, increased bladder capacity, and impaired bladder emptying resulting in increased residual urine after voiding [25]. The pathophysiology of diabetic bladder disease is multifactorial and includes detru-

sor, neuronal, urothelial, and urethral disorders [7,26]. Several animal models, including mice, rats, rabbits, cats, canines, pigs, and minipigs, have been devised to study bladder diseases [27]. However, few studies have guided clinical practice for DBD management, and larger animal models are less available due to ethical issues, laboratory facility requirements, and cost constraints [27], and thus, mice provide near ideal experimental animal models [28]. In addition, mice can be genetically manipulated to mimic almost any human disease or condition, which simplifies obtaining useful data for studies on human disease mechanisms [29]. However, it should be added that mouse models are limited by difficulties associated with measuring urine output accurately. Nonetheless, we chose to use an STZ-induced DM model for the present study.

DBD may undergo a transition from a compensated to a decompensated stage [30]. During the compensated phase, irritation associated with overactive bladder results in urgency, urge incontinence, and higher urination frequencies. However, as the disease progresses, it exhibits symptoms of decompensation, such as increased residual urine volumes, markedly reduced detrusor activity, and increased maximum bladder capacity and compliance [31]. We observed functional and structural changes in mouse bladders 12 weeks after completing the
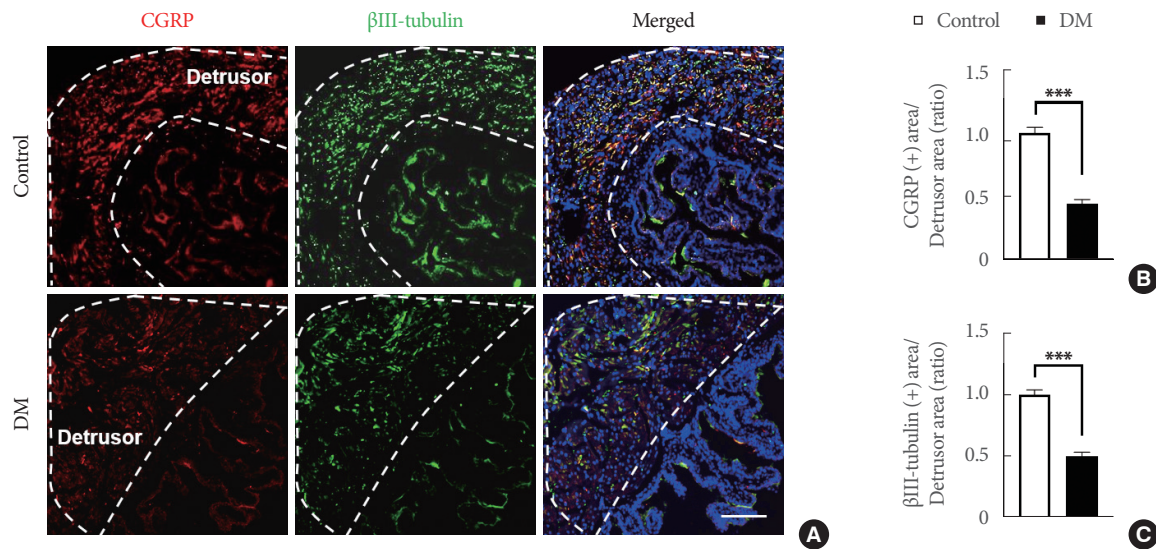
Fig. 5. Afferent nerve integrity was severely damaged in bladder detrusor muscles of streptozotocin (STZ)-induced diabetic mice (DM). (A) Calcitonin-gene related peptide (CGRP, red) and βIII-tubulin (green) immunostaining in bladder detrusor muscle (areas were measured inside the dotted lines) of an STZ-induced diabetic mouse and an age-matched control. Nuclei were labeled with 4,6-diamidino-2-phenylindole (blue). Scale bars, 100 μm. Quantification of CGRP (B) and βIII-tubulin (C) expressions in bladder detrusor muscle using Image J (National Institutes of Health, Bethesda, MD, USA). Results are presented as means ± standard error of the means (n = 4; ***P < 0.001, Student t-test). Results are presented as ratios versus controls.

5-day STZ induction period. Bladder sizes were significantly increased, and voiding frequencies significantly decreased, but maximum bladder pressures were not significantly affected, and these results are consistent with the symptoms of DBD decompensation shown in previous studies [32,33]. Therefore, we considered that STZ-induced DM at 12 weeks after induction could be used as a model for DBD, especially for DBD during the decompensated stage. Nonetheless, we suggest pathophysiologic changes in DBD at different time points in STZ-induced DM should be further investigated.

LP is a connective tissue located deep in urothelium that connects the urothelial layer with the underlying smooth muscle layer and is both blood-filled and innervated and provides nutrients and neuromediators to urothelium [34]. This layer is rich in collagen, and changes in collagen composition have been reported to contribute to symptoms of DBD [34]. For example, increased collagen levels within the LP may lead to increased tissue stiffness and strength, reduce nutrient diffusion to the urothelial layer, and lead to the symptoms of overactive bladder. Conversely, reduced collagen levels may result in tissue loss and contribute to the symptoms of underactive bladder [34,35]. Therefore, we hypothesized neurovascular units might be damaged and collagen levels reduced in the LP of DM 12

weeks after STZ-induced diabetic induction. In the current studies, frozen sections of bladder tissues were prepared, and immunofluorescent staining was performed to observe target proteins in a preliminary attempt to access the mechanism of DBD. By analyzing bladder structure, we found diabetic induction caused significant microvascular impairment, marked remodeling of LP ECM, and significantly disrupted neurogenic detrusor activity (based on efferent and afferent nerve staining results), which at least in part explained the presence of bladder dysfunction in DM. These results suggest that under diabetic conditions, reduced activity and damage to bladder efferent and afferent nerve may also be a potential cause of bladder enlargement. These results also validated our hypothesis that STZ-induced DM at 12 weeks after induction can be used as a research model for DBD and studies on DBD.

The present study has a number of limitations that should be considered. First, we assessed mice at only one timepoint; further study is needed to evaluate longitudinal changes in diabetic urinary bladder. Second, we did not investigate the signaling pathways that underlie DBD, and thus, further studies, such as next-generation sequencing analysis, are required to delineate the detailed mechanism responsible. Finally, although we attempted to measure voided volume, residual volume, voiding

efficiency, and bladder compliance in mouse bladder function test, we were unable to obtain relevant results due to the low voiding volume in mice and the inadequacy of related techniques. The development of related research equipment will be of great help to the research on DBD in mice.

AUTHOR CONTRIBUTION STATEMENT

Conceptualization: *GNY, JR*
Data curation: *MK, MC*
Formal analysis: *MK, MC, GNY*
Funding acquisition: *JR*
Methodology: *MK, MC, FL, FF, LN*
Project administration: *JR*
Visualization: *MK, MC, FL, FF, LN, GNY, JR*
Writing - original draft: *GNY*
Writing - review & editing: *JR*

ORCID

Mi-Hye Kwon   0000-0001-7100-5819
Min-Ji Choi   0000-0002-5476-356X
Fang-Yuan Liu   0000-0001-7218-6607
Fitri Rahma Fridayana   0000-0002-1478-6492
Lashkari Niloofar   0000-0001-9102-8313
Guo Nan Yin   0000-0002-2512-7337
Ji-Kan Ryu   0000-0003-0025-6025

REFERENCES

1. Yoo TK, Lee KS, Sumarsono B, Kim ST, Kim HJ, Lee HC, et al. The prevalence of lower urinary tract symptoms in population aged 40 years or over, in South Korea. Investig Clin Urol 2018;59:166-76.

2. Brown JS, Wessells H, Chancellor MB, Howards SS, Stamm WE, Stapleton AE, et al. Urologic complications of diabetes. Diabetes Care 2005;28:177-85.

3. Traish AM, Johansen V. Impact of testosterone deficiency and testosterone therapy on lower urinary tract symptoms in men with metabolic syndrome. World J Mens Health 2018;36:199-222.

4. Yuan Z, Tang Z, He C, Tang W. Diabetic cystopathy: a review. J Diabetes 2015;7:442-7.

5. Daneshgari F, Liu G, Birder L, Hanna-Mitchell AT, Chacko S. Diabetic bladder dysfunction: current translational knowledge. J Urol 2009;182(6 Suppl):S18-26.

6. Frimodt-Møller C. Diabetic cystopathy: epidemiology and related

7. Liu G, Daneshgari F. Diabetic bladder dysfunction. Chin Med J (Engl) 2014;127:1357-64.

8. Andersson KE, McCloskey KD. Lamina propria: the functional center of the bladder? Neurourol Urodyn 2014;33:9-16.

9. Cheng F, Birder LA, Kullmann FA, Hornsby J, Watton PN, Watkins S, et al. Layer-dependent role of collagen recruitment during loading of the rat bladder wall. Biomech Model Mechanobiol 2018; 17:403-17.

10. Nguyen NM, Song KM, Choi MJ, Ghatak K, Limanjaya A, Kwon MH, et al. Three-dimensional reconstruction of neurovascular network in whole mount preparations and thick-cut transverse sections of mouse urinary bladder. World J Mens Health 2021;39: 131-8.

11. Han X, Gao Y, Yin X, Wang S, Zhang X, Chen Q. Effect of electroacupuncture on bladder dysfunction via regulation of MLC and MLCK phosphorylation in a rat model of type 2 diabetes mellitus. Evid Based Complement Alternat Med 2021;2021:5558890.

12. Brown JS. Diabetic cystopathy--what does it mean? J Urol 2009; 181:13-4.

13. Hindi EA, Williams CJ, Zeef LAH, Lopes FM, Newman K, Davey MMM, et al. Experimental long-term diabetes mellitus alters the transcriptome and biomechanical properties of the rat urinary bladder. Sci Rep 2021;11:15529.

14. Yesilyurt ZE, Erdogan BR, Karaomerlioglu I, Muderrisoglu AE, Michel MC, Arioglu-Inan E. Urinary bladder weight and function in a rat model of mild hyperglycemia and its treatment with dapagliflozin. Front Pharmacol 2019;10:911.

15. Yin GN. Pericyte-derived heme-binding protein 1 promotes angiogenesis and improves erectile function in diabetic mice. Investig Clin Urol 2022;63:464-74.

16. Furman BL. Streptozotocin-induced diabetic models in mice and rats. Curr Protoc 2021;1:e78.

17. Jin HR, Kim WJ, Song JS, Choi MJ, Piao S, Shin SH, et al. Functional and morphologic characterizations of the diabetic mouse corpus cavernosum: comparison of a multiple low-dose and a single high-dose streptozotocin protocols. J Sex Med 2009;6:3289-304.

18. Yin GN, Kim DK, Kang JI, Im Y, Lee DS, Han AR, et al. Latrophilin-2 is a novel receptor of LRG1 that rescues vascular and neurological abnormalities and restores diabetic erectile function. Exp Mol Med 2022;54:626-38.

19. Mann-Gow TK, Larson TR, Wøien CT, Andersen TM, Andersson KE, Zvara P. Evaluating the procedure for performing awake cystometry in a mouse model. J Vis Exp 2017;(123):55588.

20. Arioglu Inan E, Ellenbroek JH, Michel MC. A systematic review of

urinary bladder hypertrophy in experimental diabetes: Part I. streptozotocin-induced rat models. Neurourol Urodyn 2018;37: 1212-9.

21. Miodoński AJ, Litwin JA. Microvascular architecture of the human urinary bladder wall: a corrosion casting study. Anat Rec 1999; 254:375-81.

22. Alfano M, Canducci F, Nebuloni M, Clementi M, Montorsi F, Salonia A. The interplay of extracellular matrix and microbiome in urothelial bladder cancer. Nat Rev Urol 2016;13:77-90.

23. Gabella G. Lamina propria: the connective tissue of rat urinary bladder mucosa. Neurourol Urodyn 2019;38:2093-103.

24. Mahajan PV, Subramanian S, Danke A, Kumar A. Neurogenic bladder repair using autologous mesenchymal stem cells. Case Rep Urol 2016;2016:2539320.

25. Wu L, Zhang X, Xiao N, Huang Y, Kavran M, Elrashidy RA, et al. Functional and morphological alterations of the urinary bladder in type 2 diabetic FVB(db/db) mice. J Diabetes Complications 2016;30:778-85.

26. Aizawa N, Igawa Y. Pathophysiology of the underactive bladder. Investig Clin Urol 2017;58(Suppl 2):S82-9.

27. Shen JD, Chen SJ, Chen HY, Chiu KY, Chen YH, Chen WC. Review of animal models to study urinary bladder function. Biology (Basel) 2021;10:1316.

28. Bryda EC. The Mighty Mouse: the impact of rodents on advances in biomedical research. Mo Med 2013;110:207-11.

29. Rydell-Törmänen K, Johnson JR. The applicability of mouse models to the study of human disease. Methods Mol Biol 2019;1940:3-22.

30. Daneshgari F, Liu G, Imrey PB. Time dependent changes in diabetic cystopathy in rats include compensated and decompensated bladder function. J Urol 2006;176:380-6.

31. Golbidi S, Laher I. Bladder dysfunction in diabetes mellitus. Front Pharmacol 2010;1:136.

32. Yang XF, Wang J, Rui-Wang, Xu YF, Chen FJ, Tang LY, et al. Time-dependent functional, morphological, and molecular changes in diabetic bladder dysfunction in streptozotocin-induced diabetic mice. Neurourol Urodyn 2019;38:1266-77.

33. Yang X, Lian D, Fan P, Xu Y, Wang J, Chen F, et al. Effects of Radix Linderae extracts on a mouse model of diabetic bladder dysfunction in later decompensated phase. BMC Complement Altern Med 2019;19:41.

34. Klee NS, McCarthy CG, Lewis S, McKenzie JL, Vincent JE, Webb RC. Urothelial senescence in the pathophysiology of diabetic bladder dysfunction-a novel hypothesis. Front Surg 2018;5:72.

35. Fusco F, Creta M, De Nunzio C, Iacovelli V, Mangiapia F, Li Marzi V, et al. Progressive bladder remodeling due to bladder outlet obstruction: a systematic review of morphological and molecular evidences in humans. BMC Urol 2018;18:15.